

This is the accepted manuscript made available via CHORUS. The article has been published as:

# Pair distribution function analysis: The role of structural degrees of freedom in the high-pressure insulator to metal transition of VO<sub>2</sub>

M. Baldini, P. Postorino, L. Malavasi, C. Marini, K. W. Chapman, and Ho-kwang Mao

Phys. Rev. B **93**, 245137 — Published 17 June 2016

DOI: [10.1103/PhysRevB.93.245137](https://doi.org/10.1103/PhysRevB.93.245137)

# Pair distribution function analysis: the role of structural degrees of freedom in the high pressure insulator to metal transition of VO<sub>2</sub>.

M. Baldini,<sup>1</sup> P. Postorino,<sup>2</sup> L. Malavasi,<sup>3</sup> C. Marini,<sup>4</sup> K. W. Chapman,<sup>5</sup> and Ho-kwang Mao<sup>6,7</sup>

<sup>1</sup>*Geophysical Laboratory, Carnegie Institution of Washington,*

*Advanced Photon Source, Argonne National Laboratory, Argonne, IL 60439 USA*

<sup>2</sup>*Dipartimento di Fisica, Università di Roma Sapienza, P.le A. Moro 4, 00187 Roma*

<sup>3</sup>*Department of Physical Chemistry University of Pavia and INSTM Viale Taramelli 16 27100 Pavia, Italy*

<sup>4</sup>*CELLS-ALBA, Carretera B.P. 1413, Cerdanyola del Valles, 08290, Spain*

<sup>5</sup>*X-Ray Science Division, Argonne National Laboratory,  
9700 South Cass Avenue Argonne, IL 60439, USA*

<sup>6</sup>*Geophysical Laboratory, Carnegie Institution of Washington,  
5251 Broad Branch Rd, NW Washington, DC 20015-1305*

<sup>7</sup>*Center for High Pressure Science and Technology Advanced Research,  
1690 Cailun Rd, Pudong, Shanghai, 201203, P.R. China.*

The evolution of the local structure of VO<sub>2</sub> was investigated across the pressure induced insulator to metal transition (IMT) by means of pair distribution function measurements. The pressure behavior of the V-V and V-O bond lengths have been determined. The data demonstrated that the pressure driven IMT is not activated by the suppression of the Peierls-type distortion. A clear octahedra symmetrization is observed in the metallic phase suggesting a link between structural degree of freedom and the metallization process.

PACS numbers: PACS numbers:

The microscopic mechanisms at the origin of the spectacular increase of conductivity in VO<sub>2</sub> is still elusive in spite of being the topic of many theoretical and experimental investigations for more than 50 years. The ultra-fast nature of the IMT creates several possibilities for logic and memory devices, some of which could potentially be transformative [1]. It is therefore crucial to clarify the physics governing such transition from both theoretical and applicative point of view.

The IMT is characterized by a change in the resistance of four orders of magnitude near 340 K with a simultaneous structural transition from a monoclinic insulating phase (M1) to a tetragonal (rutile) metallic phase (R) [1]. The monoclinic structure ( $P2_1/c$  space group) consists of paired V-atoms displaced out of the octahedral planes, forming V-V dimers tilted with respect to the  $a$  axis (see right panel of Fig.1). The R phase shows linear and equally spaced chains of V-atoms whereas. The electronic transition coincides with the structural changes suggesting a key role of the electron-lattice interactions. The transition is therefore ascribed to the removal of the V-V dimerization along the V-chain [2, 3]. On the other hand, theoretical and experimental evidences support the view of VO<sub>2</sub> as a Mott insulator [4–6]. Recent literature suggests that VO<sub>2</sub> should be considered a Peierls-Mott insulator where electron-electron correlations and dimerization of V ions both contribute to the opening of an insulating gap [7, 8].

VO<sub>2</sub> can assume several structural phases depending on doping, temperature and pressure. Two additional insulating phases appears on both applying uniaxial stress [9, 10] or doping [11, 12]: the monoclinic M2 phase (space group  $C2/m$ ) [13] and the triclinic (T) phase [10, 12].

An even more complex scenario has recently emerged from high pressure (HP) experiments. Indeed, an IMT is also observed applying pressure [16–18]. Optical measurements identifies the onset of this transition at around 10 GPa [16]. Transport data confirm an electronic phase transition [17] and recent results suggest that VO<sub>2</sub> is fully metallic only above 34 GPa [18]. The nature of the P-induced IMT looks remarkably different from the T-induced IMT. The relationship between the structural degrees of freedom and the electronic transition is far to be fully assessed within an exhaustive framework.

In contrast with the ambient pressure case where the metallic phase and the rutile structure are closely coupled, HP metallic VO<sub>2</sub> displays different structural properties. A new HP structural phase has been first reported at around 13 GPa by Mitrano et al. [19] and recently confirmed [18]. This new structure M1', which has not be fully determined yet, retains the  $P2_1/c$  space group and appears to be a distorted M1 structure [16, 18–20]. Above 34 GPa, an additional structural phase, named X, has been recently detected [18].

To get further insight into the HP phases of VO<sub>2</sub> and to clarify the relationship between the structural modification and the P-induced IMT, we investigate the short-range order with a challenging experiment performing X-ray total scattering measurements and atomic pair distribution function (PDF) using a diamond anvil cell [21]. An high performance experimental setup combined with a careful data analysis allowed us to determine the pressure dependence of the V-V and V-O bond distance thus providing the first experimental evidence that the removal of V-V dimers is not at the origin of the electronic transition observed at 13 GPa. Nevertheless, our PDF

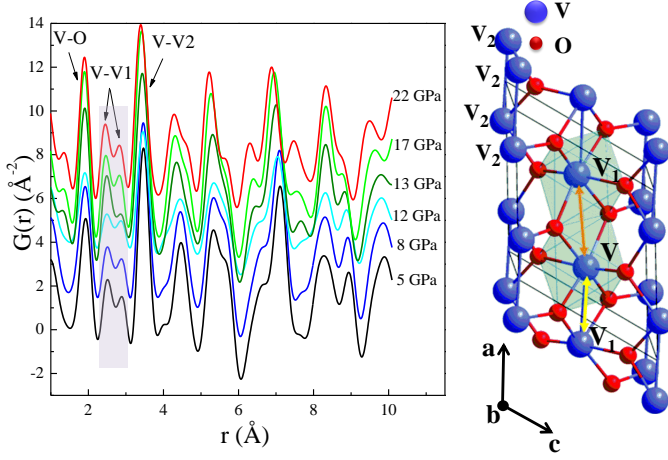


FIG. 1: Extracted  $G(r)$  as a function of pressure. The PDFs are scaled up adding a constant to facilitate data visualization. The V-V dimer bond distances are highlighted by the dashed area. The  $\text{VO}_2$  structure is reported too. Blue atoms=Vanadium, red atoms=Oxygen. The yellow and orange arrows correspond to the V-V dimer.

data suggest that a correlation between structural and the electronic degree of freedom still exists in the high pressure regime.

In order to perform high pressure PDF experiment we fully exploited the technical capabilities recently developed at beamline 11-ID-B at the Advance Photon Source at Argonne National laboratory. In particular, we took advantage of the new experimental setup that was successfully used to collect high pressure PDF data up to  $Q \geq 20 \text{ \AA}^{-1}$  [21].  $\text{VO}_2$  powder was prepared by mixing  $\text{V}_2\text{O}_3$  and  $\text{V}_2\text{O}_5$  at high temperature with argon gas flow, as described in Ref. [16]. A cross DAC with 300  $\mu\text{m}$  diamond culets and a cell seat with a 70° scattering aperture was employed [22]. The sample was dry-loaded in a 100  $\mu\text{m}$  hole. A dry loading (no pressure medium) avoids further problems in data extraction because of the pressure medium diffraction peaks. The diameter of the X-ray beam was 80  $\mu\text{m}$ . The sample pressure was estimated using the ruby fluorescence method. Total scattering data collected from an empty cell were used to perform the background subtraction. At each pressure, measurements were carried out in multiple exposures ( $\lambda = 0.137020 \text{ \AA}$ ). The 2D data sets were combined and integrated [23] and the Bragg and diffuse scattering from diamonds was identified and masked following the procedure described in ref.[21]. The corrected total scattering structure function  $S(Q)$  was obtained using standard corrections with the software PDFGETX2 [24]. The pair distribution function  $G(r)$  was extracted by directly Fourier transforming of the reduced structure function  $F(Q)$  up to  $Q_{\text{max}}$ . Reliable PDF data were obtained up

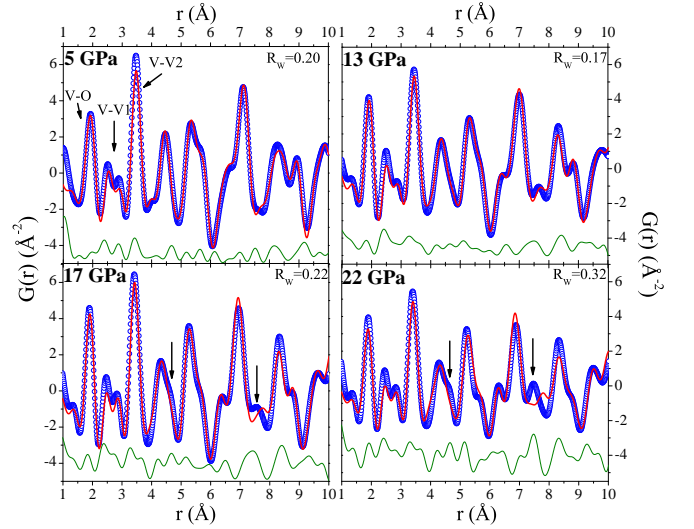


FIG. 2: PDF data at selected pressure: blue circle are used for the extracted  $G(r)$ , red line indicates the calculated  $G(r)$  and the green line is the residual (shifted down to facilitate data visualization). The black arrows in the two bottom plots indicate the PDF features that cannot be modeled using the  $P2_1/c$  space group.

to  $Q = 14 \text{ \AA}^{-1}$ . Modeling of the experimental PDF data was carried out with the aid of PDFGUI software [25].

The expected M1 structure was observed at ambient pressure with lattice parameters  $a = 5.74 \text{ \AA}$ ,  $b = 4.49 \text{ \AA}$ ,  $c = 5.39 \text{ \AA}$  and angle  $\beta = 122.6^\circ$ . In the M1 structure, the  $\text{VO}_6$  octahedra are not regular (see Fig.1) since there are two different apical V-O bonds and two short and two long equatorial V-O bonds. Because of V-V dimerization (Peiers distortion), V atoms form chains not parallel to the  $a$  axis (yellow and orange arrows in Fig.1) and two different V-V<sub>1</sub> bonds are therefore present:  $\text{V-V}_{1s} = 2.65 \text{ \AA}$  and  $\text{V-V}_{1l} = 3.12 \text{ \AA}$ .

In Fig.1, the extracted  $G(r)$ s obtained at each pressure are displayed over the 1-10  $\text{\AA}$  range. The first peak below 2  $\text{\AA}$  contains the contribution from the V-O pairs, while the two peaks observed between 2 and 3  $\text{\AA}$  correspond to the V-V<sub>1</sub> bond lengths (dashed area in Fig.1). Finally the peak around 3.5  $\text{\AA}$  contains contributions from V-V<sub>2</sub> bond lengths. No significant changes are observed for the V-O and V-V<sub>2</sub> peaks. The main and the most important evidence is that the V-V<sub>1</sub> distances remain well distinguished up to 22 GPa (as also do the relative intensities of the two peaks) demonstrating that V-V dimers still exist above the structural transition at 13 GPa (M1' phase). At ambient pressure, the T-driven IMT is characterized by the complete suppression of the V-V dimerization which takes place with the monoclinic to the rutile structural transition [1]. The P-driven metallization process does not show a strict correlation to the disappearance of the V-V dimers. As a matter of fact, most of the changes are observed above 4  $\text{\AA}$  and involve

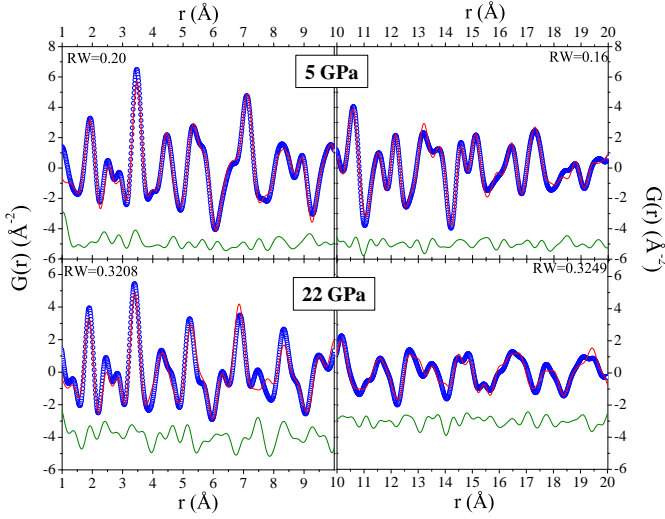


FIG. 3: Fits of the PDF data as a function of  $r$ -range. Upper plots: fits of the data collected at 5 GPa between 1-10 Å (left panel) and 10-20 Å (right panel). Bottom plots: fits of the data collected at 22 GPa between 1-10 Å (left panel) and 10-20 Å (right panel).

inter-polyhedra bond-lengths. Two shoulders appear respectively around 4.5 Å and 7.5 Å with the onset of the new  $M1'$  phase and become more preminent as pressure increases.

The PDFs of  $\text{VO}_2$  as a function of pressure were modeled with the  $M1$  structure ( $P2_1/c$ ) over the  $1 < R < 10$  Å range using lattice parameters obtained from the Rietveld refinement of the average structure. Fitted parameters were: the scale factor, the correlation parameters, lattice parameters, atomic positions, and isotropic atomic displacement. In Fig.2 the extracted  $G(r)$  (blue dots) are displayed together with the calculated  $G(r)$  (red line) for selected pressures. The  $M1$  model describes very well the features of the PDF data up to 13 GPa. Around 12-13 GPa the structural transition to the HP  $M1'$  phase takes place together with the electronic transition [16–18]. The data collected above this pressure can still be well modeled using the  $M1$  phase confirming that the  $M1'$  phase is a distorted monoclinic structure which retains the  $P2_1/c$  space group [18, 19]. However, two shoulders fail to be properly reproduced (see Fig.2). These peaks contain contributions from all the possible pairs between V and O atoms so it is not possible to identify which bond length is more affected by this structural modification.

The great advantage of PDF is the possibility of probing the local structure on different length scales by varying the range refined [26–28]. The medium-range order was investigated testing the  $M1$  model over the 10 to 20 Å  $r$ -range. Fig.3 shows fits of data Fourier transformed from using the  $P2_1/c$  space group. At 5 GPa, the agreement factor  $R_W$  decreases moving from the 1-10 Å to the 10-20 Å range (two upper plots in Fig.3). This means

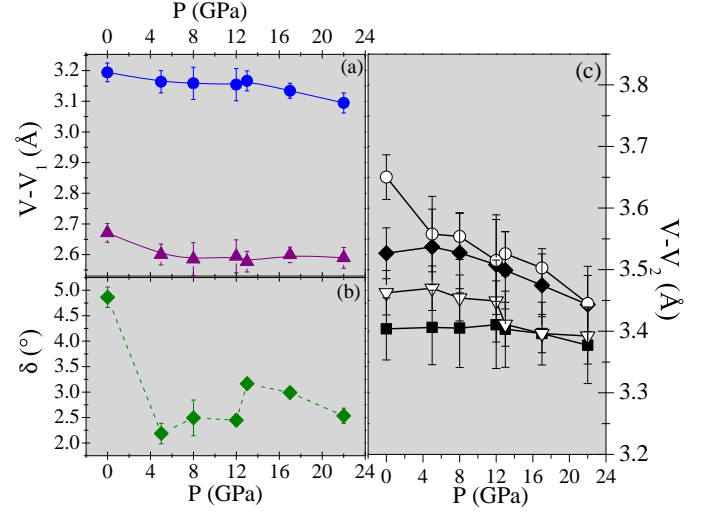


FIG. 4: Pressure dependence of the  $V-V_1$  (a), the  $V-V_2$  (c) bond lengths and  $\delta$ :  $V-V_1$  twisting angle (b).

that both medium and short-range order are characterized by the same structural features described by the  $M1$  phase. On the contrary, no improvements of the  $R_W$  factor are observed extending the  $r$ -range above 13 GPa (two bottom plots in Fig.3). The greatest discrepancies between the calculated and the measured PDFs are actually found over the 10-20 Å range. This means that the structural modifications taking place at 13 GPa mostly affect the medium range order. Several  $\text{VO}_2$  polymorph structures, in particular the  $M2$  and the  $T$  structures were then tested on the data collected above 13 GPa. The best fit was still obtained using the  $M1$  structure. Therefore we conclude that the  $P2_1/c$  model works well at the very local level ((1-10 Å)) over the entire pressure range. Pressure affects mostly the long range order structure in good agreement with previous X-ray diffraction results indicating the presence of a new distorted monoclinic phase ( $M1'$ ) closely correlated to the  $M1$  structure [18, 19].

The results of the quantitative analysis performed over the 1-10 Å range, are displayed in Fig.4 and in Fig.5. The pressure dependence of the  $V-V_1$  and  $V-V_2$  interatomic distances is shown in Fig.4(a) and (c). At ambient conditions, the  $V-V_1$  values are respectively 2.67 Å and 3.19 Å in good agreement with previous results [2, 14]. The  $V-V_1$  bond distances continuously decrease with pressure although remaining well distinguished up to 22 GPa (Fig.4(a)). In contrast with temperature and doping effect, this result unambiguously demonstrates that the  $V-V$  dimerization is not directly connected with the metalization process. The pressure dependence of the angle  $\delta$  (see Fig.4(b)) which characterizes the twisting of the  $V-V_1$  pair was also determined using the following ex-

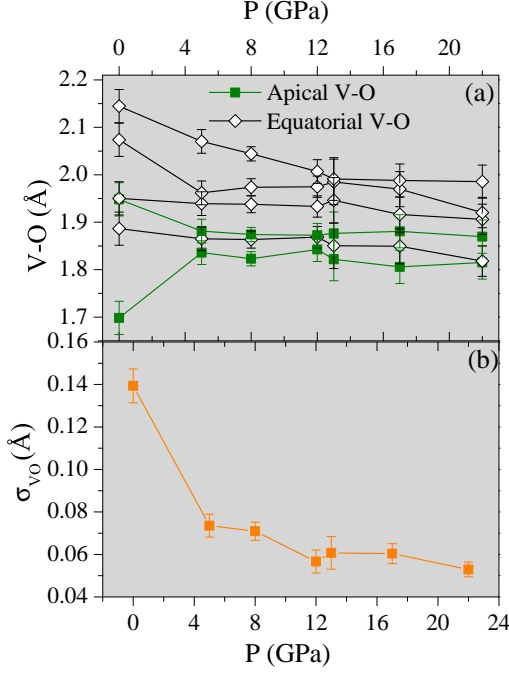


FIG. 5: Pressure dependence of the V-O interatomic distances (a) and of  $\sigma_{VO}$ : the octahedral distortion (b).

pression [2]:

$$\delta = \arccos \frac{(\frac{1}{2}R_{V-V1s})^2 + (\frac{1}{2}a)^2 - (\frac{1}{2}R_{V-V1l})^2}{2(\frac{1}{2}R_{V-V1s})(\frac{1}{2}a)}$$

where  $R_{V-V1s}$ ,  $R_{V-V1l}$ , and  $a$  values have been obtained from the 1-10 Å r-range fits. Below 5 GPa, the twisting of the V-V pairs abruptly decreases whereas a much weaker pressure dependence is observed above 5 GPa. Nevertheless, the value of  $\delta = 2.5$  at 22 GPa confirms that the V-V dimerization is far to be removed.

The pressure dependence of the V-O atomic distances is displayed in Fig.5(a). At ambient condition the  $VO_6$  octahedra are orthorhombically distorted. The V-O distances move closer to each-other with pressure, indicating a P-driven a symmetrization of the  $VO_6$  octahedra. The distortion of the  $VO_6$  was estimated using the equation reported in Ref.[14]. A more pronounced reduction of the octahedral distortion is observed between 0 and 8 GPa. The M1' phase is thus characterized by more symmetric octahedra (see Fig.5(b)). This is also consistent with the pressure dependence of the V-V<sub>2</sub> bond distances (see Fig.4(c)) which are mostly associated to structural modifications of the octahedra. This pressure behavior remarkably mimics the one observed in the V pre K-edge peaks of the system which correspond roughly to the  $e_g$  and  $t_{2g}$  contributions to the absorption [29]. This result sheds some light on the mechanism behind the IMT in  $VO_2$ . Although  $VO_2$  appears to be fully metallic only above 34 GPa in the X structural phase, HP transport data show an electronic transition

at 13 GPa with a reduction of the band gap and a resistance change of around 2 order of magnitude [17, 18] (M' phase). The M1 phase can still be used to refine the high pressure PDF data. The structural modification affects mostly the medium range order structure confirming that the M1' phase is a distorted monoclinic structure [18, 19]. Our PDF data show clearly that the  $VO_6$  octahedra are less distorted above 13 GPa and we provided the first experimental evidence that the V-V dimers are still present up to the highest pressure. The removal of the V-V dimerization is therefore not a crucial factor for inducing the electronic transition in  $VO_2$ . It was recently discovered that orbital occupation can be controlled by strain in  $VO_2$  thin films [30]. In this case, the IMT temperature is reduced by 60 K in the maximally strained sample. Strain increases the difference between the apical and the equatorial V-O bond length values leading to a change of orbital occupation and to the decrease the IMT temperature [30]. An opposite mechanism may be invoked to explain the effects of pressure on  $VO_2$ . The V-O bond distances display a closer distribution above 13 GPa, suggesting that a change in orbital occupation driven by octahedral symmetrization may be at the origin of electronic transition. The octahedral ligand-field splitting affects the hybridization strength between the V 3d and the O 2p orbitals leading to a different electronic structure arrangement.

In conclusion, we were carrying out a detailed investigation of the evolution of the local structure of  $VO_2$  up to 22 GPa using HP X-ray total scattering measurements and atomic pair distribution function. We provide the first experimental evidence that the V-V<sub>1</sub> dimerization is not suppressed up to 22 GPa. The V-V<sub>1</sub> bond distances remain well distinguished up to 22 GPa, demonstrating that the suppression of the Peierls distortion is not correlated in any way with the change of the electronic properties in the pressure range under investigation. However, at the conductive transformation around 13 GPa, structural modifications of both short and mainly medium range order do occur. The quantitative data analysis clearly shows an octahedral symmetrization which appears to be linked with the band gap reduction. We unambiguously demonstrated that the nature of the P-induced IMT is remarkably different from the T-induced IMT. This result underlines that orbital-lattice coupling plays a significant role in the pressure driven IMT and can represent a severe benchmark for any theoretical ab-initio calculation devoted to a deeper understanding of the physics of this system.

This work was supported as part of Energy Frontier Research in Extreme Environments Center (EFEE), an Energy Frontier Research Center funded by the U.S. Department of Energy, Office of Science under Award Number DE-SC0001057.

- 
- [1] Z. Yang, C. Ko, and S. Ramanathan, *Annu. Rev. Mater. Res.* 41, 337 (2011)
  - [2] T. Yao, X. Zhang, Z. Sun, S. Liu, Y. Huang, Y. Xie, C. Wu, X. Yuan, W. Zhang, Z. Wu, G. Pan, F. Hu, L. Wu, Q. Liu, and S. Wei, *PRL* 105, 226405 (2010)
  - [3] A. Cavalleri, Th. Dekorsy, H. H. W. Chong, J. C. Kieffer, and R. W. Schoenlein, *Phys. Rev. B* 70, 161102(R) (2004)
  - [4] Hyun-Tak Kim, Yong Wook Lee, Bong-Jun Kim, Byung-Gyu Chae, Sun Jin Yun, Kwang-Yong Kang, Kang-Jeon Han, Ki-Ju Yee, and Yong-Sik Lim, *PRL* 97, 266401 (2006)
  - [5] M. M. Qazilbash, M. Brehm, Byung-Gyu Chae, P.-C. Ho, G. O. Andreev, Bong-Jun Kim, Sun Jin Yun, A. V. Balatsky, M. B. Maple, F. Keilmann, Hyun-Tak Kim, D. N. Basov, *Science* 318, 1750 (2007)
  - [6] J. Cao, W. Fan, K. Chen, N. Tamura, M. Kunz, V. Eyert, and J. Wu, *Phys. Rev. B* 82, 241101(R) (2010)
  - [7] S. Biermann, A. Poteryaev, A. I. Lichtenstein, and A. Georges, *Phys. Rev. Lett.* 94, 026404 (2005).
  - [8] C. Weber, D. D. O'Regan, N. D. M. Hine, M. C. Payne, G. Kotliar, and P. B. Littlewood, *Phys. Rev. Lett.* 108, 256402 (2012).
  - [9] J. P. Pouget, H. Launois, J. P. D'Haenens, P. Merenda, and T. M. Rice, *Phys. Rev. Lett.* 35, 873 (1975).
  - [10] Joanna M. Atkin, Samuel Berweger, Emily K. Chavez, and Markus B. Raschke, Jinbo Cao, Wen Fan, and Jun-qiao Wu, *Phys. Rev. B* 85, 020101(R) (2012).
  - [11] M. Marezio, D. B. McWhan, J. P. Remeika, and P. D. Dernier, *Phys. Rev. B* 5, 2541 (1972).
  - [12] J. P. Pouget, H. Launois, T. M. Rice, P. Dernier, A. Gossard G. Villeneuve and P. Hagenmuller, *Phys. Rev. B* 10, 1801 (1974).
  - [13] Volker Eyert, *Ann. Phys.* 11, 9 (2002)
  - [14] C. Marini, S. Pascarelli, O. Mathon, B. Joseph, L. Malavasi and P. Postorino, *Europ. Phys. Lett.* 102, 66004 (2013)
  - [15] A. Tselev, I. A. Luk yanchuk, I. N. Ivanov, J. D. Budai, J. Z. Tischler, E. Strelcov, A. Kolmakov, and S. V. Kalinin, *Nano Lett.* 10, 4409 (2010)
  - [16] E. Arcangeletti, L. Baldassarre, D. Di Castro, S. Lupi, L. Malavasi, C. Marini, A. Perucchi, and P. Postorino, *Phys. Rev. Lett.* 98, 196406 (2007)
  - [17] X. Zhang, J. Zhang, F. Ke, G. Li, Y. Ma, X. Liu, C. Liu, Y. Han, Y. Ma and C. Gao, *RSC Adv.* 5, 54843 (2015)
  - [18] L. Bai, Q. Li, S. A. Corr, Y. Meng, C. Park, S. V. Sino-geikin, C. Ko, J. Wu, and G. Shen, *Phys. Rev. B* 91, 104110 (2015)
  - [19] M. Mitrano, B. Maroni, C. Marini, M. Hanfland, B. Joseph, P. Postorino, and L. Malavasi, *Phys. Rev. B* 85, 184108 (2012)
  - [20] C. Marini, E. Arcangeletti, D. Di Castro, L. Baldassarre, A. Perucchi, S. Lupi, L. Malavasi, L. Boeri, E. Pom-jakushina, K. Conder, and P. Postorino, *Phys. Rev. B* 77, 235111 (2008).
  - [21] K.W. Chapman, P. J. Chupas, G. J. Halder, J. A. Hriljac, C. Kurtz, B. K. Greve, C. J. Ruschman, A. P. Wilkinson, *J. Appl. Crystallogr.* 43, 297 (2010).
  - [22] See Supplemental Material at for more information about experimental details.
  - [23] A. P. Hammersley, S. O. Svensson, M. Hanfland, A. N. Fitch and D. Hausermann, *High Pressure Res.* 14, 235 (1996)
  - [24] Qiu, X.; Thompson, J. W.; Billinge, S. J. L., *J. Appl. Crystallogr.* 37, 678 (2004)
  - [25] Farrow, C. L.; Juhas, P.; Liu, J. W.; Bryndin, D.; Bozin, E. S.; Bloch, J.; Proffen, T.; Billinge, S. J. L., *J. Phys.: Condens. Matter* 19, 335219 (2007)
  - [26] L. Malavasi, *Dalton Trans.* 40, 3777 (2011).
  - [27] T. Egami, S. J. L. Billinge, *Underneath the Bragg peaks: structural analysis of complex materials*, Pergamon, Amsterdam; Boston, (2003).
  - [28] A. Mancini, L. Malavasi, *Chem. Comm.* 51, 16592 (2015).
  - [29] C. Marini, M. Bendele, B. Joseph, I. Kantor, M. Mitrano, O. Mathon, M. Baldini, L. Malavasi, S. Pascarelli and P. Postorino, *Eur. Phys. Lett.* 108, 36003 (2014)
  - [30] N. B. Aetukuri, A. X. Gray, M. Drouar, M. Cossale, L. Gao, A. H. Reid, R. Kukreja, H. Ohldag, C. A. Jenkins, E. Arenholz, K. P. Roche, H. A. Durr, M. G. Samant and S. S. P. Parkin, *Nature Physics* 9, 661 (2013)